Eco-evolutionary diversification of trait convergence and complementarity in mutualistic networks

Francisco Encinas-Viso[1,*], Rampal S. Etienne[2,**] and Carlos J. Melián[3,**]

1) NRCA & Centre for Australian National Biodiversity Research, CSIRO, GPO Box 1600 Canberra , Australia

2) Groningen Institute for Evolutionary Life Sciences, University of Groningen, The Netherlands

3) Department of Fish Ecology and Evolution, Center for Ecology, Evolution and Biogeochemistry, EAWAG, Swiss Federal Institute of Aquatic Science and Technology, Switzerland

Keywords: Diffuse coevolution, specialization, sexual reproduction, assortative mating, dispersal limitation, phylogenetic relatedness, obligate mutualism, morphological constraints, individual based model.

Type of Article: Letters

Number of figures: 7 (6 in color); Number of tables: 1

* Corresponding author: franencinas@gmail.com

** Joint last authorship

Empirical mutualistic networks composed by several interacting species show high levels of trait convergence and complementarity. Convergence and complementarity have been attributed to coevolutionary selection coming from both plant and animals, selection coming only from the mutualistic partners and also due to niche-based processes. Non-selective causes like traits evolving due to a Brownian motion can also produce evolutionary trait convergence and complementarity. Whether coevolutionary selection or non-selective causes are required to explain trait convergence and complementarity, the impact of population, trait and diversification dynamics on quantitative trait divergence and convergence dynamics in species-rich mutualistic networks remains largely unexplored. Here, we present a landscape genetics model to connect population, trait and diversification dynamics to study complementarity, convergence and nestedness in species-rich mutualistic networks. We compare our model to convergence and complementarity patterns observed in a plant-hummingbird mutualistic network to show that population, trait and diversification dynamics predict well plant-animal complementarity and convergence for animals but not for plants. Our analysis also shows that high levels of convergence, complementarity and nestedness are possible to predict after controlling by phylogenetic relatedness. Our results demonstrate that, in contrast to previous models based on coevolutionary selection, diversification trait dynamics requires ecological (demography and dispersal limitation), genetical (mutation, recombination and assortative mating), and morphological processes associated to trait matching to reproduce key patterns of mutualistic networks, from trait convergence and complementarity to nestedness.

Introduction

Since Darwin's book "On The Origin of Species" (Darwin, 1859), the idea of coevolution, defined as reciprocal evolutionary trait change between species, has sparked interest from biologists trying to understand how species interactions generate trait changes. The first clear indication of coevolution was Darwin's moth example (Darwin, 1862) showing that the long corolla from the orchid *Angraecum sesquispedale* could only be reached by a pollinator species with a similar or larger proboscis length. Following the moth and orchid mutualism model system, several studies have modeled coevolutionary dynamics of a few species (Ferriere *et al.*, 2007; Law *et al.*, 2001; Ferdy *et al.*, 2002; Gomulkiewicz *et al.*, 2003; Jones *et al.*, 2009), particularly highly specialized (i.e. obligatory mutualists) systems of plant-animal interactions, such as the fig-fig wasp mutualism (Bronstein *et al.*, 2006). These studies have determined the ecological conditions for coevolutionary stable systems in highly specialized plant-animal interactions (Law *et al.*, 2001; Jones *et al.*, 2009).

Janzen (1980) argued that high specialization between plants and animals was not the only example of coevolution, but coevolution can also be the product of multiple-species interactions, a term that he coined "diffuse coevolution". Diffuse coevolution means that selection on traits is determined by the interaction of more than two species and not only based on pairwise interactions. This is based on the idea of pollination or dispersal "syndromes", where plants have a set of traits that attract a specific group of pollinator or animal seed-disperser species with traits complementary to those of the plants. The idea of "diffuse coevolution" is thus linked to concepts of complementarity and convergence, and has also been related to patterns of nestedness detected across biogeographic regions in mutualistic networks.

Nestedness, defined as a non-random pattern of interactions where specialist species interact with proper subsets of more generalist species introduces the concept of "diffuse coevolution" in a more quantitative context (Bascompte *et al.*, 2003). Patterns of nestedness have been shown to provide information about the underlying network dynamics. For example, nestedness may be associated with stability and coexistence of species in mutualistic networks (Bastolla *et al.*, 2009; Okuyama & Holland, 2008), although these properties might be also independent of nestedness (Pitchford & Plank 2012).

Complementarity, trait matching between mutualistic partners (e.g. corolla length-proboscis length,

frugivore body mass-seed size, (Bascompte & Jordano, 2007)) could be the product of reciprocal evolution (i.e. coevolution). In highly specialized two-species interactions, as for example the fig-fig wasp mutualism (Bronstein *et al.*, 2006), plants coevolve with their most efficient pollinator to strengthen the complementarity of their matching adaptations (i.e., coevolutionary selection). There are also situations where an insect will be unable to reach nectar in floral tubes longer than its proboscis: the tube length sets up a barrier to some species, but not to others. For example, combining rules that link plants to pollinators whose trait ranges overlap and rules that link pollinators to flowers whose traits are below a pollinator-specific barrier value seem to predict structural properties of empirical mutualistic networks (Santamaría & Rodríguez-Gironés, 2007). Thus, developmental and morphological constraints may be required to explain complementarity (Bascompte & Jordano, 2007; Anderson *et al.*, 2010).

Convergence, the independent evolution of similar features in the same community in different evolutionary lineages is a common, perhaps a ubiquitous phenomenon but its interpretation is not clear-cut (Losos, 2011). Selective and non-selective causes can produce evolutionary trait convergence (Losos, 2011). Traits may evolve according to the same environmental or biotic pressures in independent lineages or as Brownian motion with speciation occurring randomly (Stayton, 2008). Evolutionary convergence in plant-animal mutualisms partly explains the formation of 'syndromes' produced by the presence of specific mutualist partner species (Waser *et al.*, 1996; Howe & Smallwood, 1982; Bascompte & Jordano, 2007). For example, plant species with a specific corolla morphology may determine the evolutionary convergence of pollinator species traits (Jousselin *et al.*, 2003; Guimarães *et al.*, 2011).

Recently, Guimarães *et al.* (2011) and Nuismer *et al.* (2012) explored evolutionary models using a broad range of coevolutionary selection values to study convergence and complementarity in mutualistic networks. Guimarães *et al.* (2011) show that convergence in a one-dimensional trait within a trophic level may in part emerge as a consequence of selection for a complementarity trait between trophic levels. For weak or absent coevolutionary selection, Nuismer *et al.* (2012) show that trait values in animal and plant species can be highly variable and non-convergent but positively correlated (i.e., complementary). As coevolutionary selection intensifies, variation in the trait values of animal and plant species is reduced and convergence emerges but correlations between traits of interacting

species are weakened (i.e., low pairwise complementarity). Nuismer *et al.* (2012) further explored the connection between convergence and complementarity to nestedness patterns in mutualistic networks. They showed that interactions mediated by a mechanism of phenotype matching tend to be antinested when coevolutionary selection is weak and become even more strongly antinested with increasing coevolutionary selection favoring the emergence of reciprocal specialization. Taken together, these results suggest that it is not trivial to explain simultaneously a high degree of convergence, complementarity and nestedness in species-rich mutualistic networks as observed the empirical data.

Difficulties in obtaining predictions of simultaneously large values of convergence, complementarity and nestedness in mutualistic networks may also be a consequence of unexplored drivers currently lacking in models of mutualistic networks. Most ecological models have focused on population dynamics to study nestedness while evolutionary models have focused on trait-based dynamics of interacting species, particularly the emergence of complementarity and convergence in the absence of population dynamics (Nuismer & Doebeli, 2004; Kokko & López-Sepulcre, 2007; Bascompte & Jordano, 2007; Guimarães *et al.*, 2011; Nuismer *et al.*, 2012). However, demography and trait evolution may interact to produce feedbacks and eco-evolutionary dynamics (Schoener (2011)). Yet, eco-evolutionary spatial diversification models combining simultaneously population and trait dynamics to connect trait-based patterns as complementarity and convergence with nestedness in mutualistic networks are currently lacking.

Much work on diversification emphasizes on ecological divergence and speciation (Schluter, 2009; Doebeli, 2011; Seehausen *et al.*, 2014; Rainey & Travisano, 1998; Butlin *et al.*, 2009; Gavrilets & Losos, 2009), but we propose here to step back and ask basic questions about the dynamics of divergence in mutualistic networks, and how it may depend on sexual reproduction, spatial, genetic, morphological and demographic processes. Before we understand the full impact of adaptation, coevolutionary selection and ecological speciation on evolution and diversity in ecologically complex mutualistic networks, we need to understand well the basic dynamics of mutation, gene flow, drift, morphological and spatial constraints underlying the process of diversification in species-rich mutualistic networks. Thus, to further understand the trade-offs between convergence, complementarity and nestedness in mutualistic networks, diversification models accounting for phylogenetic relatedness combining demographic, morphological constraints and evolutionary processes of trait divergence and

convergence in species-rich mutualistic networks are required. Here, we extend landscape genetics models of diversification dynamics that combine evolutionary forces (mutation, recombination and genetic drift, (Kimura, 1983; Hubbell, 2001; Lynch, 2007b; Vellend, 2010)) with demographic processes (migration, ecological drift, speciation and extinction, (Gavrilets *et al.*, 2000; de Aguiar *et al.*, 2009; Melián *et al.*, 2012; Higgs & Derrida, 1992)) to connect quantitative trait dynamics in sexually reproducing plant and pollinator populations to convergence, complementarity and nesstedness in mutualistic networks.

We find that diversification dynamics change trait distributions, and patterns of convergence, complementarity, nestedness and connectance in mutualistic networks. We show that convergence and complementarity emerge together with high levels of nestedness in the absence of coevolutionary selection. Our model predcits that trait convergence occurs mostly between the common species and on average in approximately 20% of all possible events while trait complementarity occurs in approximately 30% of all possible events. Our model predicts well plant-animal complementarity and convergence for animals but not for plants in a empirical plant-hummingbird mutualistic network. In contrast to previous studies where interactions mediated by a mechanism of phenotype matching tended to be antinested when coevolutionary selection was weak, we found that, in the absence of coevolutionary selection, highly nested values are obtained in agreement with the empirical mutualistic networks. Taken together our results suggest that diversification dynamics combining ecological (demography and dispersal limitation), population genetics (mutation, recombination, assortative mating and drift) and morphological constraints associated to trait matching expand theoretical approaches to predict the key patterns of mutualistic networks, from trait convergence and complementarity to connectance and nestedness.

The model: Eco-evolutionary diversification in mutualistic networks

We consider a landscape consisting of several individual plants (P) and animal pollinators (A). Individuals belonging to these two communities interact mutualistically and we assume obligate mutualism for both partners. Furthermore, the number of individuals at each trophic level is fixed and equal to the environmental carrying capacity for the given community. Genetic, phenotypic and

species composition change in time and space due to replacement of dead individuals by offspring of the same or another species (the key terms and model steps are summarized in figure 1 and table 1, respectively). In this section we explain how we model population, diversification and trait dynamics.

Population dynamics

Our model is a stochastic individual-based model with overlapping generations. The population consists of J_P and J_A haploid gonochoric (i.e. separated sexes) individuals with an explicit genome of size L each and equal sex ratios at the outset. The genome of each individual is composed by $L-1$ assortative mating loci and one neutral locus. Both plant and animal population reproduce sexually and are spatially structured. Demography follows by randomly selecting to die an individual plant k and animal k'. There are four conditions for producing viable offspring for the plant and animals, concerning: 1) geography, 2) genetics, 3) obligate mutualism and 4) morphology:

1. Geography: a female and a male individual within the plant and animal populations are randomly chosen among all females and males within a distance d_{max} of the dead plant k and dead animal k' . This requires two geographic distance matrices, one for plants, $D^P = [d^P_{ij}]$, and one for animals, $D^A = [d^A_{ij}]$, containing all the pairwise distances.

2. Genetics: to produce a viable offspring between the female and the male in the plant and animal populations, they must have a genetic similarity value of the assortative mating loci, $q_{♀♂}$, higher than the minimum genetic similarity to have viable offspring, q_{min}, ($q_{♀♂} > q_{min}$). This process reflects assortative mating and it requires two genetic similarity matrices, one for plants, $Q^P = [q^P_{ij}]$, and one for animals, $Q^A = [q^A_{ij}]$, containing all the pairwise similarity values.

3. Obligate mutualism: that the geographic distance between the female ♀ (animal or plant) and one of the two male animal or plant individuals, represented here as j, is lower than the maximum distance, d^{PA}_{max}, ($d^{PA}_{j♀} < d^{PA}_{max}$). This requires one geographic distance matrix, $D^{PA} = [d^{PA}_{ij}]$, containing all the pairwise distances.

4. Morphology: female plants need the presence of an animal pollinator with a larger or equally-sized proboscis than the corolla of the female plant, thus the phenotype of the selected pollinator, represented here as j, must satisfy $z^P_{♀} \leq z^A_j$. This requires two phenotype distributions,

one for the plants, $Z^P = [z_i^P]$ and one for the animals, $Z^A = [z_i^A]$. This mechanism is similar to the the "phenotypic difference" mechanism assumed in the model of Nuismer *et al.* (2012).

The offspring arising from this mating event will occupy the geographic position of the just deceased individual.

Diversification dynamics

To quantify speciation events we calculate the genetic distance between each pair of individuals based on the assortative mating loci. We represent the genome of each individual by a sequence of $L-1$ loci, where each locus can be in two allelic states, $+1$ or -1. The assortative mating loci of each plant individual i in a population of size J_P is represented as a vector: $S^i = (S_1^i, S_2^i, ..., S_L^i)$, where S_u^i is the u^{th} locus of individual i. The genetic similarity based on assortatove mating loci between individuals i and j is calculated as the sum of identical loci across the genome

$$q_{ij}^P = \frac{1}{L}\sum_{u=1}^{L} S_u^i S_u^j \tag{1}$$

where $q_{ij}^P \in \{-1, 1\}$ with the genetic similarity matrix, $Q^P = [q_{ij}^P]$, containing all pairwise genetic similarity values for plants (the same for animals, $Q^A = [q_{ij}^A]$). The genome of the offspring is obtained by a block cross-over recombination of a female genome, $S^{\female}$, and a male genome, $S^{\male}$, where a locus l in the genome of the parents is randomly chosen partitioning the genome of each individual in two blocks. All genes beyond that locus l in either genome are swapped between the two parents and eventually form two new genomes. One of the two new genomes is randomly chosen for the offspring. The offspring's genome undergoes mutations at mutation rate μ. Figure 1 describes the recombination-mutation process.

At the beginning of the simulations all individuals are genetically identical (all q_{ij}^P and $q_{ij}^A = 1$); hence they are all able to mate and produce viable offspring. The genetic similarity between individuals of a guild can be visualized as an evolutionary spatial graph (Melián *et al.*, 2010), where nodes correspond to individuals and the edges correspond to the geographic distances between a pair of individuals satisfying the genetic similarity condition for mating, $q_{ij}^P(q_{ij}^A) > q_{min}$. The connectance of the graph will decrease when generations move forward because of the processes described in

the previous section: 1) spatial constraints for mating driving assortative mating and dispersal limitation; 2) genetic divergence driven by the threshold for mating (incompatibilities), mutation and recombination forming the genome of the offspring; 3) obligate mutualistic interactions driven by spatial proximity of individuals of the other guild, and 4) morphological constraints.

These four set of processes drive genetic divergence and speciation. We followed the species definition of Nei *et al.* (1983), which states that species are groups of individuals that are reproductively isolated and can interbreed to produce fertile offspring. In our model this is realized through allowing two individuals to mate successfully if their genetic similarity value is larger or equal to the minimum value, q_{min}. Thus, speciation is defined as a group of genetically related individuals, where two individuals in a sexual population can be conspecific while also being incompatible, as long as they can exchange genes indirectly through other conspecifics (de Aguiar *et al.*, 2009; Melián *et al.*, 2010). This is the definition of 'ring species' (Moritz & Schneider, 1992).

Genetic divergence will eventually produce the formation of two genetically incompatible clusters of individuals, i.e. two species. This speciation process, also called 'fission-induced' speciation, continues to form more clusters and genetic divergence between individuals of different species increases. However, the diversification dynamics will fluctuate due to random extinctions (death of last individual of a species). A stochastic balance between speciation and extinction is eventually reached giving the final steady-state of the metacommunity.

Quantitative trait dynamics

We model each individual plant and animal with a quantitative trait, z^P and z^A, respectively. The processes described in figure 1 govern two quantitative traits, one for each guild: proboscis or bill length (z_i^A) in pollinators and corolla length (z_i^P) in plants. The quantitative trait of offspring is determined by the additive genetic effects of the genome (i.e. no epistasis) after the process of randomly choosing one of the new two genomes and mutation (figure 1) plus a normally distributed environmental effect, ϵ, $\mathcal{N}(\mu_\epsilon = 0, \sigma_\epsilon^2 = 1)$ (Guimarães *et al.*, 2011). The phenotype of the plant offspring i is $z_i^P = g_i^P + \epsilon$ and the genetic component (g_i^P) of the phenotype of offspring i is

$$g_i^P = L + S_o^i \tag{2}$$

with $S_o^i = \sum_{u=1}^{L} S_u^i$. Hence g_i^P is calculated as the sum of alleles across the genome (Kondrashov & Shpak, 1998) plus the number of loci to avoid negative trait values (g_i^A is calculated similarly for animals). We assumed that the magnitude of the influence (i.e., effect sizes) of any given locus on this quantitative trait is equal across all the loci (Seehausen *et al.*, 2014). This means that two individuals with a different combination of alleles in the genome can express the same quantitative trait (Losos, 2011).

Neutral locus evolution

We considered a neutral locus to estimate genetic divergence among species for the calculation of convergent events (see section "Evolutionary convergence"). The neutral locus is located at the end of the genome at the position L and has k possible allelic states. The locus is completely unlinked from the rest of the genome that contains the assortative mating loci. We used low mutation rates for this neutral locus, $\mu_{neutral} = 10^{-7}$, and the k allele mutation model (i.e. model in which each allele can mutate to any of the other k–1 possible alleles with equal probability (Hoban *et al.* (2013)). We used the Cavalli-Sforza distance to calculate the matrix of genetic distances among species (Cavalli-Sforza & Edwards (1967)).

Convergence, complementarity and nestedness

Evolutionary convergence

The calculation of convergence requires computing pairwise genotypic and phenotypic similarities and the similarity between mean species phenotypes from distantly related species. With only three species, only one convergence is possible after excluding the sister species (see figure 2). The number of convergences potentially increases with the number of species present. For example, if we have ten species and we exclude one of them as the sister species of the focal species, we have nine species to calculate convergence. If we find that two out of nine species are phenotypically similar enough to the focal species, we count two (out of nine,$\sim$ 22%) convergences. We repeat this by changing the focal species and calculate the mean convergence events over all species. In contrast to previous approaches that used the mean pair-wise difference between traits of species (Guimarães *et al.*, 2011)

or the variance of species traits in a guild as a proxy to predict convergence (i.e., large values weak convergence whereas small values of the variance may indicate strong convergence, (Nuismer *et al.*, 2012)), we used the relationship between genetic divergence and phylogenetic relatedness for the estimation of evolutionary convergences. The advantage of our method considering phylogenetic relatedness is that it excludes cases of development of very similar trait values from sister species (i.e., parallel evolution, (Losos, 2011)) and therefore it does not overestimate convergence events. Finally, to visualize the genetic relatedness between species we constructed clustering trees using Euclidean distance with the Python library ETE 2.01 (Huerta-Cepas *et al.*, 2010)).

Phenotypic similarity

The phenotypic similarity for plants (p_{ij}^P) between individual i and j is defined as

$$p_{ij}^P = 1 - \frac{|z_i^P - z_j^P|}{z_{max}^P} \tag{3}$$

where z_i^P and z_j^P are the phenotypic similarity values of i and j, respectively, and z_{max}^P is the maximum value of the phenotype distribution, Z^P . Thus, the elements $p_{ij}^P \in \{0, 1\}$ of the phenotypic similarity matrix, $\mathcal{P}^P = [p_{ij}^P]$ represent all pairwise values for plants (the same for animals, $\mathcal{P}^A = [p_{ij}^A]$).

Mean genetic and phenotypic species similarity

We define evolutionary convergence as the similarity between average species phenotypes from distantly related species. We assume that two species are distantly related, in phylogenetic terms, if they do not come from a direct common ancestor, i.e. they are not sister species. To exclude sister species from the analysis we need to calculate the mean genetic similarity among species of the same guild. The mean genetic similarity between a plant species k and a plant species l is

$$\hat{q}_{kl}^P = \frac{1}{n_k n_l} \sum_{i=1}^{n_k} \sum_{j=i}^{n_l} q_{ij}^P \tag{4}$$

where q_{ij}^P is the genetic similarity between an individual i of plant species k and an individual j of plant species l, and n_k and n_l are the absolute abundances of plant species k and l, respectively. The elements $\hat{q}_{kl}^P$ form the matrix $Q_s^P = [\hat{q}_{kl}^P]$ from which the sister species of each species in the guild can

be identified (The elements for animals, $Q_s^A = [\hat{q}_{kl}^A]$, are calculated in the same way as we did for the plants). To calculate evolutionary convergence we need to know the average phenotypic similarity between two species. We define phenotypic similarity between species k and l as

$$\hat{p}_{kl}^P = \frac{1}{n_k n_l} \sum_{i=1}^{n_k} \sum_{j=i}^{n_l} p_{ij}^P \tag{5}$$

which is analogous to the definition of eq. 4, but now considering phenotypes instead of genotypes. This will build a species phenotypic similarity matrix $P_s^P = [\hat{p}_{kl}^P]$ (the species phenotypic similarity matrix, $P_s^A = [\hat{p}_{kl}^A]$, is calculated analogously for the animals). We then focus on each species in turn and exclude its sister species to avoid cases of parallel evolution to calculate the number of convergences related to the focal species. We define a focal plant species k and a non-sister plant species l to be convergent if phenotypic similarity between them is higher than between focal and sister species ($\hat{p}_{k,sister}^P < \hat{p}_{kl}^P$) and higher than a certain phenotypic threshold value t_{conv} ($\hat{p}_{kl}^P > t_{conv}$); convergent species is calculated analogously for the animals).

Evolutionary complementarity

Evolutionary complementarity does not require the genetic similarity matrix. We only need to estimate the phenotypic similarity between plant and animal species and we do this as we did for the evolutionary convergence. We calculate the phenotypic similarity matrix $P_s^{PA} = [\hat{p}_{kh}^{PA}]$. This matrix contains the mean trait similarity for each plant species k and animal species h. The condition for complementarity is that the similarity between a plant species k and an animal species h is $\hat{p}_{kh}^{PA} > t_{comp}$, where t_{comp} is the phenotypic threshold value to detect a complementarity event.

Plant-animal interactions

In addition to the genetic and geographic constraints for mating, we consider two other conditions for plants and animals: obligate mutualism and morphological constraints. Obligate mutualism applies to the plants and animals to reproduce but the morphological constraints only apply to plants. We therefore need a geographic distance matrix, D^{PA}, to describe the geographic distance between plant and animal individuals. Plant-animal mutualistic interactions are here described as follows: plants benefit from the presence of specific pollinators that are able to pollinate them and animals benefit

from the presence of plants that provide resources for them. Thus, we have two extra conditions for mating:

1. Female plants need the presence of an animal pollinator (i.e., male and female represented as j) within a close distance, $d^{PA}_{j\varphi} < d^{PA}_{max}$. The pollinator must have a larger or equally-sized proboscis than the corolla of a plant, $z^{P}_{\varphi} \leq z^{A}_{j}$. This corresponds to a morphological constraint for individual interactions observed between plant and pollinator species (Stang *et al.*, 2009, 2006).

2. Animals need the presence of a plant (male or female represented as j) within a close geographic distance, $d^{PA}_{jk} < d^{PA}_{max}$.

Our model allows bookkeeping of who is interacting with whom, i.e. this means we can record exactly which plant and animal individuals are interacting. This bookkeeping enables us to identify the consequences of geography, genetics, obligate mutualism and morphology for the evolution and final topology of the network. We record the identity of the mutualistic partners during the reproduction process for plants and animals after reaching the steady-state to reconstruct the plant-animal interaction network.

Nestedness and connectance

To study the connection between convergence and complementarity with network properties, we measured two topological properties of plant-animal mutualistic networks: nestedness and connectance. We estimated nestedness using the NODF algorithm developed by (Almeida-Neto *et al.*, 2008) because of its statistical robustness. NODF is based on standardized differences in row and column fills and paired matching of occurrences. Connectance measures the proportion of realized interactions among all possible interactions in a network. It is defined as $C = \frac{k}{P*A}$, where k represents the number of realized interactions between plant and animal species and P and A represent the number of plant and animal species in the network, respectively (Jordano *et al.*, 2003).

Simulations

We simulated equal population sizes for plants and animals with $J^P = J^A = 1,000$ individuals. Genome size, L, of each individual was 150 loci. Initial trait distributions for the plants, $Z^P = [z_i^P]$ and animals, $Z^A = [z_i^A]$, were generated following equation 2 plus a normally distributed environmental effect, ϵ, $\mathcal{N}(\mu_\epsilon = 0, \sigma_\epsilon^2 = 1)$. To ensure plant mating conditions are met at the beginning of the simulation all animal individuals have a higher phenotypic trait value that the plant individuals.

Geographic distances between each pair of individuals i and j for the plants, d_{ij}^P, and animals, d_{ij}^A, were calculated as follows: 1) Euclidean coordinates of a two-dimensional space (x_i, y_i) were sampled from a uniform distribution ($x_i = [0, 1], y_i = [0, 1]$) for each individual for the plants and animals; 2) Using these coordinates we calculated a matrix of relative Euclidean distances between the individuals for the plants, d_{ij}^P, and animals, d_{ij}^A. This procedure was repeated for each of the geographic distance matrices (D^{PA}, D^P, D^A).

We ran 2,000 generations for each replicate for a total of 500 replicates, where a generation is the update of the effective population size ($J^P = J^A = 1,000$), i.e. the number of steps equal to the effective population size. Steady-state was verified by checking the constancy of speciation events during the last 100 generations. We calculated convergence, complementarity, nestedness and connectance at steady-state. Convergence and complementarity events were calculated for a whole range ($[0.0, 1.0]$) of their respective thresholds, t_{conv} and t_{comp}. We explored parameter combinations with mutation rate, $\mu \in \{10^{-4}, 10^{-2}\}$, minimum genetic similarity, $q_{min} = 0.97$, maximum distance for finding a mate and disperse, $d_{max} \in \{0.1, 0.3\}$, and a maximum geographic distance to find a mutualistic partner, $d_{max}^{PA} = 0.3$. We implemented the model in Python (and tested in IPython (Pérez & Granger, 2007)). Plots were produced using the Python library Matplotlib (Hunter, 2007).

Model-data fitting

We test our model's predictions of convergence and complementarity using a dataset of a plant-hummingbird network containing morphological and phylogenetic data (Maglianesi *et al.* (2014)). We used empirical values of corolla length and bill length from plants and hummingbirds, respectively. To calculate convergence with this empirical dataset we also considered the phylogenetic relationships

among species. We used a well resolved phylogeny of hummingbirds from McGuire *et al.* (2007). We used 24 hummingbird species from a total of 38, which were not present in the phylogenetic tree. For the plant species we constructed a phylogenetic tree using genetic data of 69 species from genBANK and calculate a ML tree using RAXML . We excluded 64 plant species from the analysis (see Suppl. Materials) because their phylogenetic relationships were not well resolved (polytomies), leaving a total of 69 species from a total of 133 from the dataset of Maglianesi et al (2014). We used the R package APE (Paradis *et al.*, 2004) in R (R Core Team, 2013) to visualize and prune the tips (species) that were not used in our anlaysis (see Suppl. Materials)

We used the phylogenetic trees with their respective branch lengths to calculate a genetic distance matrix among species. Using both phylogenetic tress (hummingbirds and plants) we simulated nucleotide sequences of 100bp with the program SeqGen *(Rambaut & Grassly, 1997)* following the Juke-Cantor model of molecular evolution. These simulated sequences were then used to calculate the genetic distance matrix using the R package *seqinr* in R (R Core Team, 2013). To compare the convergence values obtained from the empirical data with our model predictions, we generated 1000 replicates from the simulations (bootstrapping) with each replicate containing the same number of plant and animal species as the empirical data. Mean values as well 0.05 and 0.95 CI were generated from these 1000 replicates. Complementarity and convergence were calculated for each of the replicates across the whole range of convergence, t_{conv}, and complementarity, t_{comp}, thresholds. In the absence of simulated phenotypic data for extinct species we could not calculate together the most recent common ancestor and phenotypic values to estimate convergence following metrics by Stayton (2015). Instead, results presented in figure 7 for convergence events were calculated assuming a conservative estimation meaning the 30% of the most genetically similar species and not only the sister species to the focal species were excluded.

Results

Population dynamics and diversification dynamics changed plant and animal community trait distributions (i.e. corolla and proboscis lengths) with bimodal distributions being the most commonly produced patterns across replicates (figure 3). At species level, a gradient of species phenotypes

with common species presenting lower mean and higher variance than rare species emerged. Mean and variance of the trait values were correlated for most replicates (Spearman-$\rho > 0.41$, $p < 0.05$) and the distributions of abundance for plant or animal species were highly skewed and significantly different from a normal distribution (Lilliefors's test, all $p < 0.001$). Abundance predicted plant or animal mean species traits in approximately 70% of the replicates (Spearman-$\rho > 0.32$, $p < 0.05$) and trait variance for all replicates ($0.39 <$ Spearman-$\rho < 0.79$, all $p < 0.05$). Mean and variance of species trait values significantly differed between common and rare plant or animal species (inset in figure 3) suggesting a strong impact of diversification by producing a gradient of species phenotypes in mutualistic networks.

Evolutionary convergence events occurred in all replicate simulations (see equations 4 and 5 with an example of evolutionary convergence events in animals and plants represented in figure 4). Convergence events were heterogeneously distributed across species with most events occurring between common species ($0.42 <$ Spearman-$\rho < 0.89$, all $p < 0.05$). Evolutionary convergence occurred on average in $17.3 \pm 6\%$ of all possible convergence events with more than 95% of these events occurring within the three most common species. These results show that evolutionary convergence is not randomly distributed across pairs of species but highly aggregated during the diversification process. Evolutionary convergence can also be visualized using a scatter plot of the genotype-phenotype map for all pairs of individuals within the plant and animal communities (figure 5). As expected from equation 2, there is a positive genotype-phenotype relationship. The scatter plot contains three main clouds of points that consistently occur in our simulations for the plants, P, and animals, A: 1) pairs of individuals of the same species with high genetic ($q_{ij} > q_{min}$) and phenotypic ($p_{ij} > 0.9$) similarity, 2) pairs of individuals of the same species with genetic similarity below q_{min} ($q_{ij} < q_{min} = 0.97$) and high phenotypic similarity ($p_{ij} > 0.9$). These are incompatible individuals for mating, yet with high phenotypic similarity, $p_{ij} > 0.9$, and 3) highly genetically dissimilar individuals from different species, $q_{ij} \ll q_{min}$, but with the presence of highly phenotypically similar individuals ($p_{ij} > 0.9$). This last category shows evidence of evolutionary convergence between species in plants and animals. An increase in mutation rate increases the genetic divergence between species, as expected, but it does not change the genotype-phenotype relationship qualitatively (see figure 5).

Evolutionary complementarity occurred with a similar frequency as evolutionary convergence in

each replicate (see equation 5 and compare the initial with the final trait distributions in figure 3), but with a larger variation ($20 \pm 18\%$). Connectance values were consistently medium or high ($\overline{C} = 0.5 \pm 0.07$, figure 6), mostly larger than reported in empirical data where it ranges between 0.05-0.25. Nestedness values were always high ($\overline{N} = 69.97 \pm 13.4$ (figure 6)), as observed in the empirical plant-pollinator networks. Convergence, complementarity and nestedness did not show signs of trade-offs and were uncorrelated across all replicates ($0.08 <$ Spearman-$\rho < 0.27$, all $p > 0.1$) with the exception of a positive correlation between trait complementarity and evolutionary convergence in the plant community (Spearman-$\rho = 0.61$, all $p < 0.05$). Our results, using phylogenetically relatedness and phenotypic similarity for the estimation of evolutionary convergence and complementarity in the absence of coevolutionary selection, show evolutionary trait convergence and complementarity in all our replicate simulations but with little and large variation, respectively. For weak or absent coevolutionary selection, trait convergence in plant and animal communities is largely independent or positively correlated with trait complementarity for the animal and plant community, respectively. Our predictions consistently show low to medium convergence and complementarity together with high levels of nestedness in the absence of coevolutionary selection and convergence-complementarity trade-offs.

Our model predicts well plant-animal complementarity and convergence for animals but not for plants in a empirical plant-hummingbird mutualistic network (figure 7). The observed proportion of complementarity events for the empirical plant-hummingbird data is within the CI for a broad range of values of the complementarity threshold, t_{comp} (figure 7a). Our model consistently predict higher proportion of convergence events than the observed proportion in the plant community (figure 7b). Predictions in the proportion of convergent events quickly increase for a high convergence threshold value (red lines figure 7b) and saturates around the same observed values for medium and low convergent threshold values. These results suggest that in the absence of coevolutionary selection among plants and hummingbirds our model predicts higher proportion of convergence events than the observed number in the plant community. Predictions of the proportion of convergence events for the hummingbird community are within the estimated CI for all the range of convergence threshold values (figure 7c). These results show that predictions for plant-animal complementarity and convergence in the hummingbird community are robust against a broad range of threshold values suggesting that

there is not need to invoke coevolutionary selection to predict these observed patterns.

Discussion

In the present study, we have extended previous landscape genetics models (de Aguiar *et al.*, 2009; Melián *et al.*, 2012) to connect population and diversification dynamics with quantitative trait dynamics to study trait complementarity, convergence and nestedness in species-rich mutualistic networks. Our results show high levels of nestedness combined with low to medium levels of convergence and complementarity after controlling for phylogenetic relatedness (figure 2). This partly deviates from the simultaneously high levels of nestedness, convergence and complementarity observed in empirical data across a broad range of biogeographic regions (Bascompte & Jordano, 2007). After controlling for phylogenetic relatedness and phenotypic similarity, we show that evolutionary trait convergence is observed in all our replicates with little variation ($17.3 \pm 6\%$) and it is heterogeneously distributed across species with most events occurring between the common species. This suggests that evolutionary convergence is not randomly originated across pairs of species but highly aggregated during the diversification process. Similarly, complementarity is consistently observed but with a larger variation than convergence $20 \pm 18\%$. Our analysis suggests that convergence, complementarity and nestedness do not necessarily have to show signs of trade-offs in the absence of coevolutionary selection. Our results also show predictions that match the observed plant-animal complementarity and convergence for animals but not for plants in a empirical plant-hummingbird mutualistic network. These results suggest that weak or absent coevolutionary selection may reproduce the observed patterns of convergence in the hummingbird community analyzed here. We predict higher proportion of convergent events than the observed proportion in the plant community and we would expect even stronger deviations under strong coevolutionary selection because it tends to predict higher proportion of convergence events than weal coevolutionary selection. This means there is a need to invoke additional mechanisms to explain the observed patterns of convergence in the plant community here explored.

Previous studies have argued that evolutionary convergence is the product of multispecific coevolutionary processes ('diffuse coevolution')(Janzen, 1980; Thompson & Cunningham, 2002; Jordano

et al., 2003; Bascompte & Jordano, 2007) and therefore convergence events are molded by similar ecological (or niche) selective pressures. Recent mutualistic coevolutionary models assuming the mechanism of 'phenotypic difference' (as our model) have shown that for weak or absent coevolutionary selection trait values in animal and plant species can be highly variable and non-convergent, but trait values of animal and plants species show high complementarity (i.e. they are positively correlated) (Nuismer *et al.*, 2012). As coevolutionary selection intensifies, variation in the trait values of animal and plant species is reduced and convergence increases, but correlations between traits of interacting species are weakened (i.e., low pairwise complementarity). However, Guimarães *et al.* (2011) have shown that trait convergence may in part emerge as a consequence of selection for a complementarity trait between the plants and animals. These approaches used all the species (Guimarães *et al.*, 2011) or the variance as a proxy to predict convergence (i.e., large values weak convergence whereas small values of the variance may indicate strong convergence, (Nuismer *et al.*, 2012)) and they might overestimate convergence events because they do not consider phylogenetic relatedness. Using phylogenetic relatedness and phenotypic similarity for the estimation of evolutionary convergences in the absence of coevolutionary selection, we show that evolutionary trait convergence and complementarity is observed in all our replicate simulations but with little and large variation, respectively. Our results contrasts with previous findings (Nuismer *et al.*, 2012) that under weak or absent coevolutionary selection we always find convergence and these convergence values are largely independent of the degree of trait complementarity between plant and animals for the animals, but positively correlated between plant and animals for the plant community.

Interestingly, the mechanism of plant-animal interaction considered in our model, where the trait of the animal needs to be equal or larger than the trait of plant ('phenotypic difference'), has shown to make unlikely the evolution of convergence and complementarity by coevolutionary selection (Nuismer *et al.*, 2012). However, our model shows that by considering non-selective processes it is possible to observe the evolution of both convergence and complementarity. It remains to be seen whether the action of both (selective an non-selective forces) will be able to generate the observed patterns of high convergence, complementarity and nestedness in species-rich mutualistic networks.

Non-selective forces underlying trait dynamics can produce convergence. For example, Stayton (2008) simulated evolution along phylogenies according to a Brownian motion model of trait change

and demonstrated that rates of convergence can be quite high when clades are diversifying under only the influence of genetic drift. Furthermore, other type of constraints in the production of variation can also lead to convergence. If the variation produced is limited, then unrelated species are likely to produce the same variation, which may then become fixed in the population by genetic drift (Stayton, 2008; Losos, 2011). This may be common feature of biological systems because DNA contains only four possible states for a given nucleotide position, and therefore it is likely that distantly related taxa will independently acquire the same change by chance regardless of the environmental conditions or niche-driven dynamics (Losos, 2011). Developmental constraints or the evolution of genetic networks by non-adaptive processes may also be explanations for the convergence of traits (Solé *et al.*, 2002; Lynch, 2007a; Losos, 2011), but the role of developmental constraints or genetic networks in determining convergence in species-rich mutualistic networks has yet not been explored. For example, the tinkering of traits by evolutionary forces largely affects developmental pathways (e.g. gene regulatory networks) (Solé *et al.*, 2002). Developmental pathways are not static but can diverge through time randomly without substantially affecting the phenotype (Wagner, 2008). This concept, also called developmental system drift (DSD) (True & Haag, 2001), might play an important role in the evolution of convergence in morphological traits and it should be considered as another process where drift can act (Ohta, 2002), for example, by random wiring in gene regulatory networks. Our results based on a method that excludes cases of the development of a similar trait in related but distinct species descending from the same ancestor (i.e., parallel evolution, (Losos, 2011)) show that additional constraints such as dispersal limitation, obligate mutualisms and assortative mating limit the production of variation and lead consistently to convergence in species-rich mutualistic networks.

Evolutionary complementarity is also consistently observed in our results but with a larger variation than convergence. Complementarity is argued to be the main result of tight coevolution between mutualistic species by mechanisms, such as trait-matching (e.g. corolla length-proboscis length) (Jordano *et al.*, 2003). There is empirical (Anderson & Johnson, 2008) and theoretical evidence (Gomulkiewicz *et al.*, 2000) for coevolutionary hot spots (Thompson, 1999), which suggests that local selective regimes can promote the coevolution of traits (Gomulkiewicz *et al.*, 2000; Ferdy *et al.*, 2002; Gomulkiewicz *et al.*, 2003; Jordano *et al.*, 2003; Bronstein *et al.*, 2006; Thompson & Cunningham, 2002; Thompson, 2009; Jones *et al.*, 2009). In contrast, our results show that low to medium levels of

complementarity can emerge from relatively non-selective forces and constraints occurring at several levels, from geographic limits to encounter partners and disperse to the genetic and morphological constraints to producing viable offspring. In addition, our model-data fitting show our predictions fit well to the observed plant-hummingbird complementarity across a broad range of complementarity threshold values (figure 7).

Our model predicts that the distribution of traits, regardless of species differences, generally evolves towards a bimodal distribution of phenotypes. This result was previously obtained by Kondrashov & Shpak (1998), who studied a model in the absence of selection and with assortative mating in a infinite population. Their result with strong assortative mating produces high correlations of allelic effects among all loci, which leads to the evolution of two phenotypic classes: one with alleles increasing the trait and the other with alleles decreasing the trait (Crow & Kimura, 1970). Devaux & Lande (2008) found similar results using a finite diploid population with multiple alleles per locus and they showed that the splitting of the phenotype distribution is possible under strong assortative mating and genetic drift, but the distribution is transient rather than permanent. In our model the distribution is not transient, and this may be probably due to having only considered two allelic states in our assortative mating loci, instead of multiple allelic states, for each locus. As Devaux & Lande (2008) explained, by assuming a normal distribution of allelic effects at each locus we could obtain a more continuous unimodal (i.e. normal) distribution of phenotypes. We need further analytical exploration to thoroughly understand the determinants of trait distributions in our model. Nevertheless, we find a gradient of species phenotypes from low to high mean trait values (Insets in figure 3), but trait distributions for the parameter combination explored are not right-skewed, as observed in real plant-pollinator communities (Stang *et al.*, 2009). This might be due to the influence of other traits not considered in our model, such as forbidden links (e.g. body size) and developmental constraints.

Nuismer *et al.* (2012) explored the connection between convergence and complementarity to nestedness patterns in mutualistic networks. They show that coevolutionary selection tend to decrease nestedness and it generates even more strongly antinested networks when coevolutionary selection increases by favoring the emergence of reciprocal specialization. In contrast, nestedness values were very high in our model, as in real mutualistic networks. Previous neutral models taking into account

ecological drift (Krishna *et al.*, 2008; Canard *et al.*, 2012), produced high values of nestedness which suggests that random interactions and species abundance distribution ('neutral forbidden links' (Canard *et al.*, 2012)), are determinants of the structure of mutualistic networks. Connectance values obtained from our simulations are close to the predictions of other neutral network models (Canard *et al.*, 2012). However, compared to real mutualistic networks with similar diversity as ours (24 plant and animal species on average), our connectance values ($\overline{C} = 0.5$) are higher than the reported webs ($C = 0.28$) (Olesen & Jordano, 2002). Interestingly, Nuismer *et al.* (2012) found that only assuming coevolutionary selection forces also leads to an increase in connectance. This means that both basic genetic and ecological processes and coevolutionary selection can increase connectance in mutualistic networks. The question is why observed mutualistic webs have a lower connectance than those predicted by our model and those considering coevolutionary selection. We conjecture that this difference in connectance values might be due to different types of forbidden links (i.e. biological constraints impeding plant-animal interactions), such as phenology (Encinas-Viso *et al.*, 2012; Olesen *et al.*, 2008), body size (Olesen *et al.*, 2010)or environmental fluctuations that were not explicitly included in our approach.

High values of the required genetic similarity to produce viable offspring, q_{min}, and shorter geographical distances for mating (d_{max}) lead to higher species diversity in models with one metacommunity (Melián *et al.*, 2012), but low geographic distances for mating could decrease species diversity due to the difficulty of finding mates (i.e., Allee effect) or due to inbreeding, especially for high genetic similarity threshold values to produce viable offspring. In our model we assume that genetic incompatibilities, assortative mating and morphological traits are determined by the same multiple loci (i.e. they have the same genetic basis) and these genes show pleiotropic effects. We do not explicitly model how incompatibilities accumulate (Welch, 2004) and assortative mating and morphological traits are calculated in a similar way: we sum genetic differences regardless of the magnitude of the influence (i.e., effect sizes) of any given locus on this quantitative trait (Seehausen *et al.*, 2014). This means that two individuals with different combinations of alleles in the genome can express the same quantitative trait (Losos, 2011). Our interpretation of non-random mating and an ecological trait may be similar to the concept of 'magic' traits (Thibert-Plante & Gavrilets, 2013). A 'magic' trait combines a trait subject to divergent selection and another trait related to nonrandom mating (i.e.

reproductive isolation) that are pleiotropic expressions of the same gene(s) (Servedio *et al.*, 2011). There are other alternatives for the relationship between assortative mating and the morphological trait (Servedio *et al.*, 2011). For instance, assortative mating and the morphological trait may be determined by different sets of genes and express different levels of pleiotropic effects (i.e. a partial 'magic' trait (van Doorn & Weissing, 2001)). One might also explore further the influence of the morphological constraint on the evolution of traits. In our model, this constraint might be exerting weak selection on the plant traits because some pollinator individuals may be able to interact with a larger number of plants. The comparison with other models without any morphological constraint (i.e. only non-random mating) and with morphological constraints for animals and plant reproduction (i.e. phenotypic matching) might elucidate the importance of morphological constraints in the evolution of mutualistic networks.

In summary, our results show the emergence of convergence, complementarity and nestedness following basic genetic and ecological processes. We did not find high levels of convergence and complementarity but our predictions fit well to the observed plant-hummingbird complementarity and hummingbird convergence. In contrast to previous studies showing antinested networks when considering coevolutionary selection, we found that, in the absence of coevolutionary selection, highly nested values are obtained in agreement with the empirical mutualistic networks (Bascompte *et al.*, 2003). Our results suggest that diversification dynamics combining ecological (demography and dispersal limitation), population genetics (mutation, recombination, assortative mating and drift) and morphological constraints may form the basic processes producing the key patterns of mutualistic networks, from trait convergence and complementarity to connectance and nestedness. More generally, our model shows that it is important to consider non-selective forces to explain broad evolutionary patterns and the emergence of community structure in species-rich interacting networks.

Acknowledgments

We thank Martina Stang and Ole Seehausen for useful discussions. FEV and RSE were supported by grants from the Netherlands Organization for Scientific Research (NWO). CJM was supported by the Swiss National Science Foundation (SNSF-project 31003A-144162).

MyRefNumbers

References

MyRefNumbers1.

Almeida-Neto, M., aes, P. G., aes, P. G., Loyola, R. & Ulrich, W. (2008). A consistent metric for nestedness analysis in ecological systems: reconciling concept and measurement. *Oikos*, 117, 1227–1239.

MyRefNumbers2.

Anderson, B. & Johnson, S. (2008). The geographical mosaic of coevolution in a plant-pollinator mutualism. *Evolution*, 62, 220–225.

MyRefNumbers3.

Anderson, B., Terblanche, J. S. & Ellis, A. G. (2010). Predictable patterns of trait mismatches between interacting plants and insects. *BMC Evolutionary Biology*, 10, 204.

MyRefNumbers4.

Bascompte, J. & Jordano, P. (2007). Plant-animal mutualistic networks: The architecture of biodiversity. *Annu. Rev. Ecol. Evol. Syst.*, 38, 567–593.

MyRefNumbers5.

Bascompte, J., Jordano, P., Melian, C. J. & Olesen, J. M. (2003). The nested assembly of plant-animal mutualistic networks. *Proc. Natl. Acad. Sci. USA*, 100, 9383–9387.

MyRefNumbers6.

Bastolla, U., Fortuna, M., Pascual-García, A., Ferrera, A., Luque, B. & Bascompte, J. (2009). The architecture of mutualistic networks minimizes competition and increases biodiversity. *Nature*, 458, 1018–1020.

MyRefNumbers7.

Bronstein, J. L., Alarcon, R. & Geber, M. (2006). The evolution of plant-insect mutualisms. *New Phytol.*, 172, 412–428.

MyRefNumbers8.

Butlin, R., Bridle, J. & Schluter, D. (2009). *Speciation and Patterns of Diversity*. Cambridge: Cambridge University Press. 346 p.

MyRefNumbers9.

Canard, E., Mouquet, N., Marescot, L., Gaston, K., Gravel, D. & Mouillot, D. (2012). Emergence of structural patterns in neutral trophic networks. *Plos One*, 7, e38295.

MyRefNumbers10.

Cavalli-Sforza, L. L. & Edwards, A. W. (1967). Phylogenetic analysis. models and estimation procedures. *Am J Hum Genet.*, 19, 233–257.

MyRefNumbers11.

Crow, J. & Kimura, M. (1970). *An introduction to population genetics theory*. Harper & Row Publishers, New York.

MyRefNumbers12.

Darwin, C. (1859). *On the origin of the species*. Murray.

MyRefNumbers13.

Darwin, C. (1862). *Fertilisation of Orchids*. Murray.

MyRefNumbers14.

de Aguiar, M., Baranger, M., Baptestini, E., Kaufman, L. & Bar-Yam, Y. (2009). Global patterns of speciation and diversity. *Nature*, 460, 384–387.

MyRefNumbers15.

Devaux, C. & Lande, R. (2008). Incipient allochronic speciation due to non-selective assortative mating by flowering time, mutation and genetic drift. *Proc R Soc B*, 275, 2723–2732.

MyRefNumbers16.

Doebeli, M. (2011). *Adaptive diversification*. Princeton University Press, Princeton, NJ.

642 MyRefNumbers17.
643 Encinas-Viso, F., Revilla, T. & Etienne, R. (2012). Phenology drives mutualisic network structure
644 and diversity. *Ecol Lett*, 15, 198–208.

645 MyRefNumbers18.
646 Ferdy, J., Despres, L. & Godelle, B. (2002). Evolution of mutualism between globeflowers and
647 their pollinating flies. *Journal of Theoretical Biology*, 217, 219–234.

648 MyRefNumbers19.
649 Ferriere, R., Gauduchon, M. & Bronstein, J. L. (2007). Evolution and persistence of obligate mu-
650 tualists and exploiters: competition for partners and evolutionary immunization. *Ecology Letters*,
651 10, 115–126.

652 MyRefNumbers20.
653 Gavrilets, S., Acton, R. & Gravner, J. (2000). Dynamics of speciation and diversification in a
654 metapopulation. *Evolution*, 54, 1493–1501.

655 MyRefNumbers21.
656 Gavrilets, S. & Losos, J. (2009). Adaptive radiation: Contrasting theory with data. *Science*, 323,
657 732–737.

658 MyRefNumbers22.
659 Gomulkiewicz, R., Nuismer, S. L. & Thompson, J. N. (2003). Coevolution in variable mutualisms.
660 *The American Naturalist*, 162, S80–S93.

661 MyRefNumbers23.
662 Gomulkiewicz, R., Thompson, J. N., Holt, R. D., Nuismer, S. L. & Hochberg, M. E. (2000). Hot
663 spots, cold spots, and the geographic mosaic theory of coevolution. *The American Naturalist*, 156,
664 156–174.

665 MyRefNumbers24.
666 Guimarães, P., Jordano, P. & Thompson, J. (2011). Evolution and coevolution in mutualistic
667 networks. *Ecol Lett*, 14, 877–885.

668 MyRefNumbers25.

669 Higgs, P. & Derrida, B. (1992). Genetic distance and species formation in evolving populations. *J*
670 *Mol Evol*, 35, 454–465.

671 MyRefNumbers26.

672 Hoban, S., Gaggiotti, O., Consortium, C. & Bertorelle, G. (2013). Sample planning optimization
673 tool for conservation and population genetics (spotg): a software for choosing the appropriate
674 number of markers and samples. *Methods in Ecology and Evolution*, 4, 209–303.

675 MyRefNumbers27.

676 Howe, H. & Smallwood, J. (1982). Ecology of seed dispersal. *Ann Rev. Ecol. Syst.*, 13, 201–228.

677 MyRefNumbers28.

678 Hubbell, S. (2001). *The unified neutral theory of biodiversity and biogeography*. Princeton University
679 Press, Princeton, NJ.

680 MyRefNumbers29.

681 Huerta-Cepas, J., Dopazo, J. & Gabaldón, T. (2010). Ete: a python environment for tree explo-
682 ration. *BMC Bioinformatics*, 11, 24.

683 MyRefNumbers30.

684 Hunter, J. (2007). Matplotlib: A 2d graphics environment. *Computing In Science & Engineering*,
685 9, 90–95.

686 MyRefNumbers31.

687 Janzen, D. (1980). When is it coevolution? *Evolution*, 34, 611–612.

688 MyRefNumbers32.

689 Jones, E., Ferrière, R. & Bronstein, J. (2009). Eco-evolutionary dynamics of mutualists and
690 exploiters. *Am Nat*, 174, 780–794.

691 MyRefNumbers33.

692 Jordano, P., Bascompte, J. & Olesen, J. (2003). Invariant properties in coevolutionary networks
693 of plant-animal interactions. *Ecol. Lett.*, 6, 69–81.

694 MyRefNumbers34.

695 Jousselin, E., Rasplus, J.-Y. & Kjellberg, F. (2003). Convergence and coevolution in a mutualism:
696 evidence from a molecular phylogeny of ficus. *Evolution*, 57, 1255–1269.

697 MyRefNumbers35.

698 Kimura, M. (1983). *The neutral theory of molecular evolution*. Cambridge University Press,
699 Cambridge, UK.

700 MyRefNumbers36.

701 Kokko, H. & López-Sepulcre, A. (2007). The ecogenetic link between demography and evolution:
702 can we bridge the gap between theory and data? *Ecology Letters*, 10, 773–782.

703 MyRefNumbers37.

704 Kondrashov, A. & Shpak, M. (1998). On the origin of species by means of assortative mating.
705 *Proc. R. Soc. Lond. B*, 265, 2273–2278.

706 MyRefNumbers38.

707 Krishna, A., Guimarães, P., Jordano, P. & Bascompte, J. (2008). A neutral-niche theory of
708 nestedness in mutualistic networks. *Oikos*, 117, 1609–1618.

709 MyRefNumbers39.

710 Law, R., Bronstein, J. L. & Ferrière, R. (2001). On mutualists and exploiters: plant-insect coevo-
711 lution in pollinating seed-parasite systems. *Journal of Theoretical Biology*, 212, 373–389.

712 MyRefNumbers40.

713 Losos, J. (2011). Convergence, adaptation, and constraint. *Evolution*, 65, 1827–1840.

714 MyRefNumbers41.

715 Lynch, M. (2007a). The evolution of genetic networks by non-adaptive processes. *Nature Reviews*
716 *Genetics*, 8, 803–813.

717 MyRefNumbers42.

718 Lynch, M. (2007b). The frailty of adaptive hypotheses for the origins of organismal complexity.
719 *Proc Natl Acad Sci USA*, 104, 8597–8604.

MyRefNumbers43.

Maglianesi, M., Bluthgen, N., Böhning-Gaese, K. & Schleuning, M. (2014). Morphological traits determine specialization and resource use in plant-hummingbird networks in the neotropics. *Ecology*, 95, 3325–3334.

MyRefNumbers44.

McGuire, J., Witt, C., Altshuler, D. & Remsen, J. (2007). Phylogenetic systematics and biogeography of hummingbirds: Bayesian and maximum likelihood analyses of partitioned data and selection of an appropriate partitioning strategy. *Syst. Biol.*, 56, 837–856.

MyRefNumbers45.

Melián, C. J., Alonso, D., Allesina, S., Condit, R. & Etienne, R. (2012). Does sex speed up evolutionary rate and increase biodiversity? *PloS Comput Biol*, 8, e1002414.

MyRefNumbers46.

Melián, C. J., Alonso, D., Vázquez, D., Regetz, J. & Allesina, S. (2010). Frequency-dependent selection predicts patterns of radiations and biodiversity. *PLoS Comput Biol*, 6, e1000892.

MyRefNumbers47.

Moritz, C. & Schneider, C. J. (1992). Evolutionary relationships within the *Ensatina eschscholtzii* complex confirm the ring species interpretation. *Syst Biol*, 41, 273–291.

MyRefNumbers48.

Nei, M., Maruyama, T. & Wu, C.-I. (1983). Models of evolution of reproductive isolation. *Genetics*, 103, 557–579.

MyRefNumbers49.

Nuismer, S. & Doebeli, M. (2004). Genetic correlations and the coevolutionary dynamics of three-species systems. *Evolution*, 58, 1165–1177.

MyRefNumbers50.

Nuismer, S. L., Jordano, P. & Bascompte, J. (2012). Coevolution and the architecture of mutualistic networks. *Evolution*, 67, 338–354.

MyRefNumbers51.

Ohta, T. (2002). Near-neutrality in evolution of genes and gene regulation. *Proc Natl Acad Sci USA*, 99, 16134–16137.

MyRefNumbers52.

Okuyama, T. & Holland, J. N. (2008). Network structural properties mediate the stability of mutualistic communities. *Ecol. Lett.*, 11, 208–216.

MyRefNumbers53.

Olesen, J., Bascompte, J., Dupont, Y., Elberling, H., Rasmussen, C. & Jordano, P. (2010). Missing and forbidden links in mutualistic networks. *Proc. R. Soc. Lond. B.*

MyRefNumbers54.

Olesen, J. & Jordano, P. (2002). Geographic patterns in plant-pollinator mutualistic networks. *Ecology*, 89, 2416–2424.

MyRefNumbers55.

Olesen, J. M., Bascompte, J., Elberling, H. & Jordano, P. (2008). Temporal dynamics in a pollination network. *Ecology*, 89, 1573–1582.

MyRefNumbers56.

Paradis, E., Claude, J. & Strimmer, K. (2004). Ape: analyses of phylogenetics and evolution in r language. *Bioinformatics*, 20, 289–290.

MyRefNumbers57.

Pérez, F. & Granger, B. (2007). IPython: a System for Interactive Scientific Computing. *Comput. Sci. Eng.*, 9, 21–29.

MyRefNumbers58.

R Core Team (2013). *R: A Language and Environment for Statistical Computing*. R Foundation for Statistical Computing, Vienna, Austria. URL `http://www.R-project.org/`.

MyRefNumbers59.

Rainey, P. & Travisano, M. (1998). Adaptive radiation in a heterogeneous environment. *Nature*, 394, 69–72.

MyRefNumbers60.

Rambaut, A. & Grassly, N. (1997). Seq-gen: An application for the monte carlo simulation of dna sequence evolution along phylogenetic trees. *Computer Applications In The Biosciences*, 13, 235–238.

MyRefNumbers61.

Santamaría, L. & Rodríguez-Gironés, M. A. (2007). Linkage rules for plant-pollinator networks: trait complementarity or exploitation barriers? *PLoS Biol*, 5, e31.

MyRefNumbers62.

Schluter, D. (2009). Evidence for ecological speciation and its alternative. *Science*, 323, 737–741.

MyRefNumbers63.

Schoener, T. W. (2011). The newest synthesis: understanding the interplay of evolutionary and ecological dynamics. *Science*, 331, 426–429.

MyRefNumbers64.

Seehausen, O., Butlin, R. K., Keller, I., Wagner, C. E., Boughman, J. W., Hohenlohe, P. A., Peichel, C. L., Saetre, G. P. *et al.* (2014). Genomics and the origin of species. *Nature Reviews Genetics*, 15, 176–192.

MyRefNumbers65.

Servedio, M., Kopp, G. V. M., Frame, A. & Nosil, P. (2011). Magic traits in speciation: 'magic' but not rare? *Trends Ecol Evol*, 26, 389–399.

MyRefNumbers66.

Solé, R., Ferrer-Cancho, R., Montoya, J. & Valverde, S. (2002). Selection, tinkering, and emergence in complex networks. *Complexity*, 8, 20–33.

MyRefNumbers67.

Stang, M., Klinkhamer, P. & van der Meijden, E. (2006). Size constraints and flower abundance determine the number of interactions in a plant-flower visitor web. *Oikos*, 112, 111–121.

MyRefNumbers68.

Stang, M., Klinkhamer, P., Waser, N., Stang, I. & van der Meijden, E. (2009). Size-specific

interaction patterns and size matching in a plant-pollinator interaction web. *Ann Bot*, 103, 1459–1469.

MyRefNumbers69.

Stayton, C. T. (2008). Is convergence surprising? An examination of the frequency of convergence in simulated datasets. *J. Theo. Biol.*, 252, 1–14.

MyRefNumbers70.

Stayton, C. T. (2015). The definition, recognition, and interpretation of convergent evolution, and two new measures for quantifying and assessing the significance of convergence. *Evolution*, 69, 2140–2153.

MyRefNumbers71.

Thibert-Plante, X. & Gavrilets, S. (2013). Evolution of mate choice and the so-called magic traits in ecological speciation. *Ecology letters*, 16, 1004–1013.

MyRefNumbers72.

Thompson, J. N. (1999). Specific hypotheses on the geographic mosaic of coevolution. *The American Naturalist*, 153, S1–S14.

MyRefNumbers73.

Thompson, J. N. (2009). The coevolving web of life. *The American Naturalist*, 173, 125–140.

MyRefNumbers74.

Thompson, J. N. & Cunningham, B. M. (2002). Geographic structure and dynamics of coevolutionary selection. *Nature*, 417, 735–738.

MyRefNumbers75.

True, J. R. & Haag, E. S. (2001). Developmental system drift and flexibility in evolutionary trajectories. *Evolution & Development*, 3, 109–119.

MyRefNumbers76.

van Doorn, G. & Weissing, F. (2001). Ecological versus sexual models of sympatric speciation: a synthesis. *Selection*, 2, 17–40.

826 MyRefNumbers77.

827 Vellend, M. (2010). Conceptual synthesis in community ecology. *The Quarterly Review of Biology*,
828 85, 183–206.

829 MyRefNumbers78.

830 Wagner, A. (2008). Neutralism and selectionism: a network-based reconciliation. *Nature Reviews*
831 *Genetics*, 9, 965–974.

832 MyRefNumbers79.

833 Waser, N., Chittka, L., Price, M., Williams, N. & Ollerton, J. (1996). Generalization in pollination
834 systems, and why it matters. *Ecology*, 77, 1043–1060.

835 MyRefNumbers80.

836 Welch, J. J. (2004). Accumulating Dobzhansky-Muller incompatibilities: Reconciling theory and
837 data. *Evolution*, 58, 1145–1156.

Table 1: Glossary of mathematical notation and parameter values

Notation	Definition	Values
J^P, J^A	Effective population size of plants (P) and animals (A)	1,000
d_{ij}^P, d_{ij}^A	Geographical pairwise distance plants (P) and animals (A)	variable
d_{max}	Maximum geographical distance to mate and disperse	0.3
D^P, D^A	Geographic distance matrix with all d_{ij}^P and d_{ij}^A values	variable
d_{ik}^{PA}	Geographical distance between plant i and animal k	variable
d_{max}^{PA}	Maximum geographical distance to find a mutualistic partner	0.3
D^{PA}	Geographic distance matrix with all the d_{ik}^{PA} values	variable
q_{ij}^P, q_{ij}^A	Genetic similarity between ind. i and j in (P) and (A)	variable
Q^P, Q^A	Genetic similarity matrix with all the q_{ij}^P and q_{ij}^P values	variable
q_{min}	Minimum genetic similarity to have viable offspring	0.97
z_i^P, z_i^A	Quantitative trait of ind. i in (P) and (A)	variable
Z^P, Z^A	Quantitative trait distribution in (P) and (A)	variable
p_{ij}^P, p_{ij}^A	Phenotypic similarity between ind. i and j in (P) and (A)	variable
$\mathcal{P}^P, \mathcal{P}^A$	Phenotypic similarity matrix with all the p_{ij}^P and p_{ij}^A values	variable
L	Size of the genome	150
g_i^P, g_i^A	Genetic component of phenotype of offspring in (P) and (A)	variable
ϵ	Environmental component of phenotype of offspring	$\mathcal{N}(0,1)$
μ	Mutation rate per locus	$10^{-4} - 10^{-2}$
$\hat{q}_{kh}^P, \hat{q}_{kh}^A$	Mean genetic simil. between species k and h in (P) and (A)	variable
Q_s^P, Q_s^A	Species genetic simil. matrix with all $\hat{q}_{kl}^P$ and $\hat{q}_{kl}^A$ values	variable
$\hat{p}_{kh}^P, \hat{p}_{kh}^A$	Mean phen. simil. between species k and h in (P) and (A)	variable
P_s^P, P_s^A	Species phen. simil. matrix with all $\hat{p}_{kl}^P$ and $\hat{p}_{kl}^A$ values	variable
$\hat{p}_{kh}^{PA}$	Mean trait similarity plant species k and animal species h	variable
P_s^{PA}	Phenotypic simil. matrix with all $\hat{p}_{kh}$ values	variable
${}^h conv$	Phenotypic threshold to calculate convergence events	variable
${}^h comp$	Phenotypic threshold to calculate complementarity events	variable

Tables

Figures

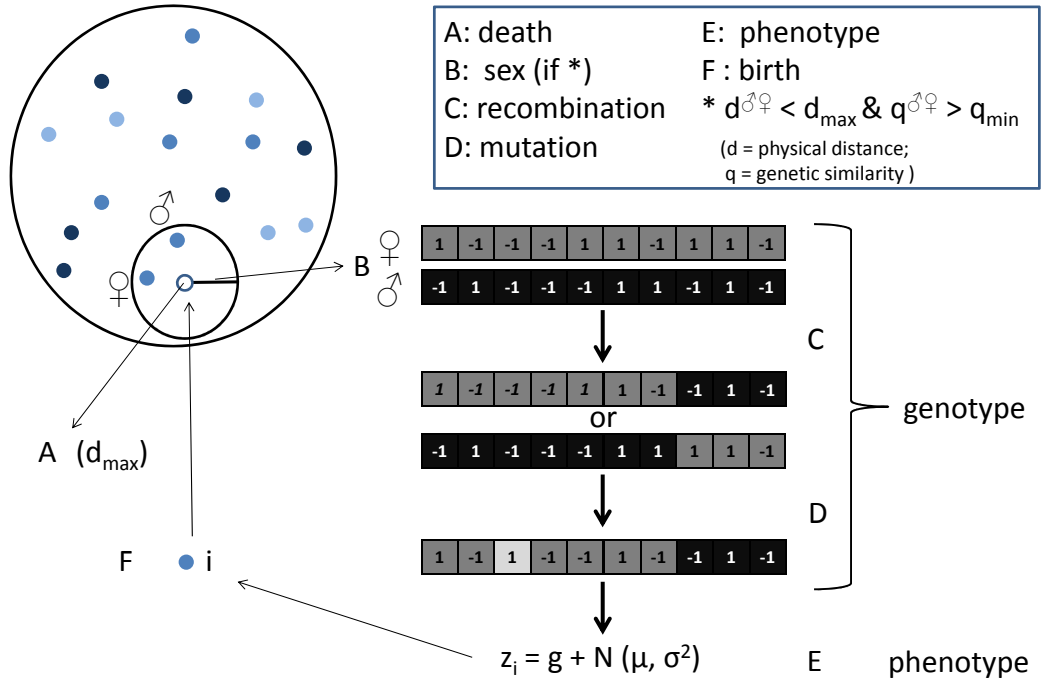

Figure 1: This figure summarizes the death-birth cycle per time step. Individuals are represented as filled circles and blue tones represent variation of phenotypes. (A) an individual k is randomly selected to die and leaves an empty location in the landscape. (B) a female individual, ♀, is randomly selected among all females satisfying the condition $d_{k♀} < d_{max}$. We then choose randomly a male, ♂, among all males satisfying $d_{k♂} < d_{max}$ and $q_{♀♂} > q_{min}$ with q_{min}, the minimum genetic similarity required for mating. In addition to these two constraints, two more are required to complete mating. For the condition of obligate mutualism, the geographic distance between the female (animal or plant), and an animal (or plant) individual j, must satisfy $d^{PA}_{j♀} < d^{PA}_{max}$. Finally, female plants need the presence of an animal pollinator with a larger or equally-sized proboscis than the corolla of the female plant, thus individual pollinators represented as j, must satisfy $z_{♀_P} \leq z_{j_A}$. In (C) and (D) we calculate the genome of the new offspring once these constraints are satisfied. (C) Genomes are composed of L loci where each locus can be in two allelic states $(-1, 1)$ and undergo block crossover recombination between female (dark gray) and male (black). A position l in the genome of the parents is randomly chosen partitioning the genome in two blocks. All genes beyond the l locus in either organism's genome is swapped between two parents and two new genomes are formed. (D) One of the two new genomes is randomly chosen for the offspring i, S^i_o, and it might undergo mutation (light gray). (E) The phenotype expression of offspring i is $z_i = g_i + \epsilon$ with $g_i = L + S^i_o$ and ϵ are the genetic and environmental component of the phenotype, respectively. (F) The offspring i occupies the site of the dead individual k.

Q_s matrix

	a	b	c
a		0.85	0.97
b			0.89
c			

P_s matrix

	a	b	c
a		0.98	0.90
b			0.92
c			

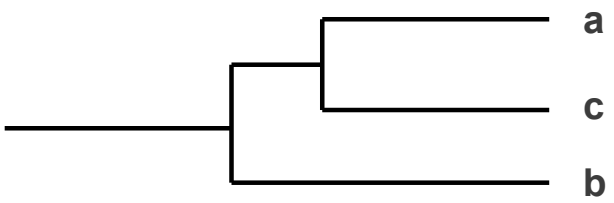

Figure 2: This figure illustrates a simple example of evolutionary convergence using species a, b and c. The upper matrix ($Q_S = [\hat{q}_{kl}]$) shows species a and c are genetically closely related, $\hat{q}_{ac} = 0.97$, while genetically distant from species b ($\hat{q}_{ab} = 0.85$, $\hat{q}_{cb} = 0.89$). A clear description of these genetic relationships can be represented with a cluster tree or dendrogram, as shown in the lower part of the figure. Thus, we establish that species a and c are sister species. The species phenotypic similarity matrix, $P_S = [\hat{p}_{kh}]$ shows that species a and b are phenotypically highly similar ($\hat{p}_{ab} = 0.98$) and highly genetically dissimilar ($\hat{q}_{ab} = 0.85$) (i.e. more than the average intraspecific genetic similarity or sister species 0.97), indicating an event of evolutionary convergence.

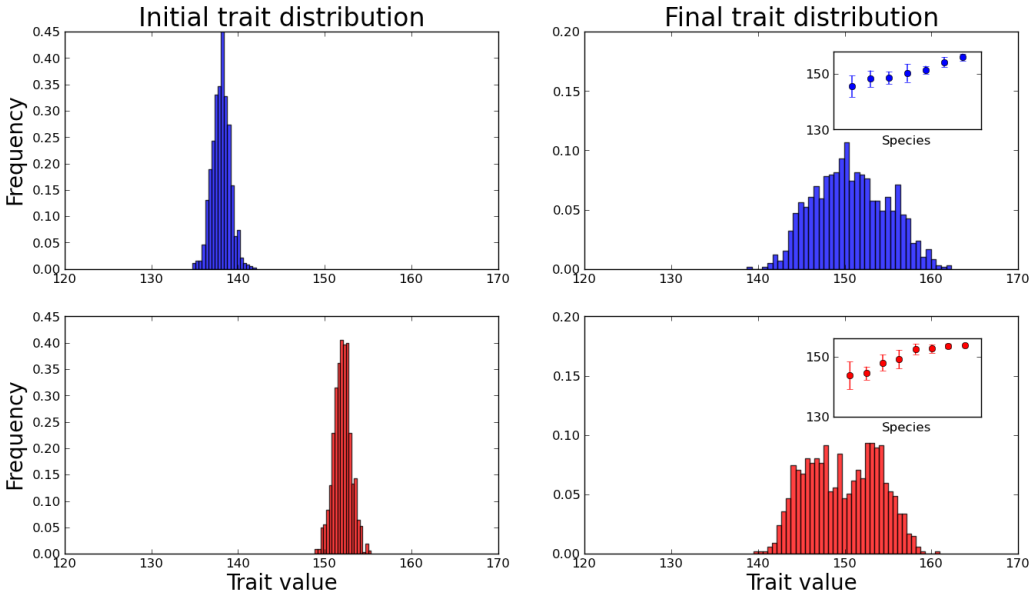

Figure 3: Changes in trait distribution of plants (top, blue) and animals (bottom, red). Left and right panels show the initial and final trait distribution, respectively. The insets in the right panels show the mean trait and standard error for each species sorted from the most common to the most rare. Initial trait distributions changed towards higher variance, and in most replicates, towards bimodal distribution in both guilds. Plot shows the outputs from one replicate with parameters values $q_{min} = 0.97$**,** $d_{max} = d_{max}^{PA} = 0.3$**,** $\mu = 5 \times 10^{-3}$ **and** $J_P = J_A = 1,000$**.**

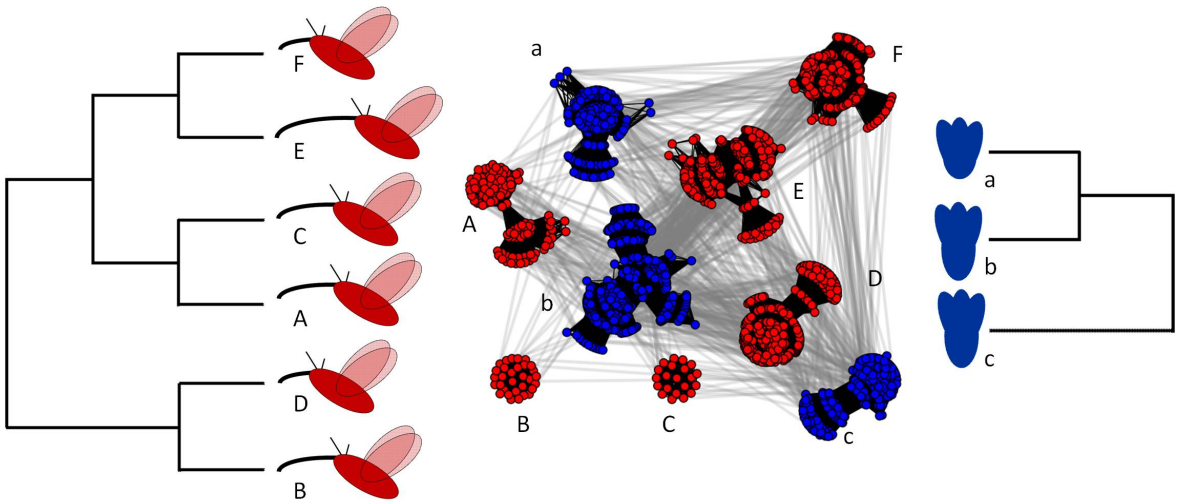

Figure 4: Evolutionary convergence and complementarity in plant-pollinator networks. Trees at the left and right side show genetic similarities between animal (red) and plant (blue) species, respectively. Mean species trait, proboscis and corolla length, is sketched with cartoons next to their respective position in the trees. Animals, composed by six species, have two evolutionary convergence events (A-B and F-D). Plants, composed by three species, have one convergent event (b-c). The central part of the figure shows the network of plant-animal interactions, where each node (colored filled circles) represents an individual. The network is composed of two types of links: genetic relatedness links (black solid) forming clusters that represent species and plant-animal individual-based interaction links (gray). The network shows variability in terms of genetic relatedness and plant-animal interactions within a species (i.e. high intraspecific variability). This figure is an example from one replicate simulation. Parameters used are as in figure 3, $q_{min} = 0.97$**,** $d_{max} = d^{PA}_{max} = 0.3$**,** $\mu = 5 \times 10^{-3}$ **and** $J^P = J^A = 1,000$**.**

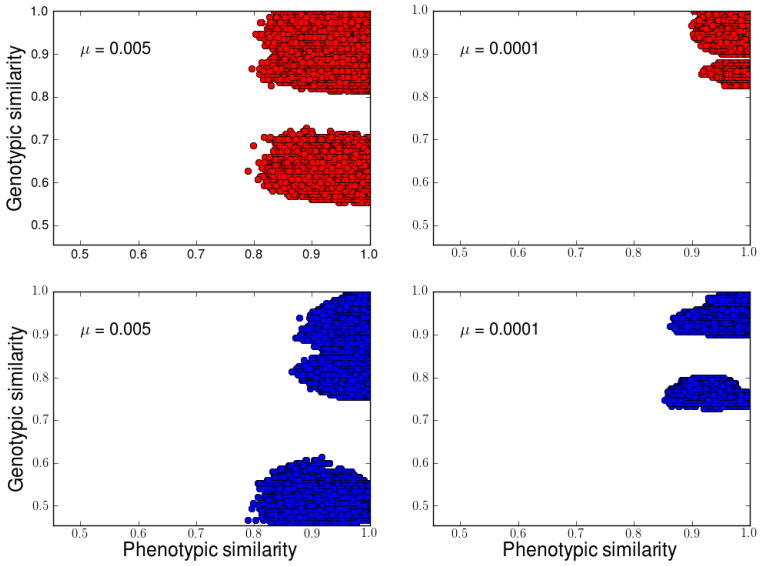

Figure 5: The effect of mutation rate on the genotype-phenotype relationship. Top and bottom panels show the genotype-phenotype relationship for animals (red) and plants (blue), respectively. Right panels show the genotype-phenotype relationship for mutation rate $\mu = 5 \times 10^{-3}$ and left panels for $\mu = 10^{-4}$. Each plot is a scatter plot, where each filled circle represents phenotypic and genetic similarity between two individuals of a particular guild (plant or animal) from one replicate. Individuals with high phenotypic similarity and genetic dissimilarity suggests evolutionary convergence of traits, regardless of mutation rate. Parameters used are $q_{min} = 0.97$, $d_{max} = d^{PA}_{max} = 0.3$ and $J_P = J_A = 1,000$.

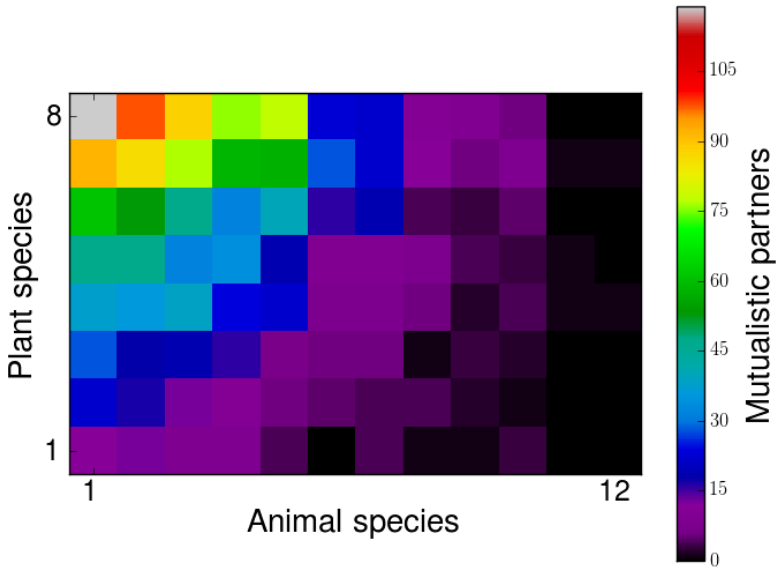

Figure 6: Plant-animal species interaction network. Plant species are represented in rows and animal species in columns. The color gradient indicates the number of mutualistic partners (i.e. individuals interacting) shared between plant and animal species. This matrix comes from one replicate with nine plant and thirteen animal species. The network shows high level of nestedness ($N = 0.72$) and intermediate level of connectance ($C = 0.5$). Parameters used are $q_{min} = 0.97$, $d_{max} = d^{PA}_{max} = 0.3$, $\mu = 5 \times 10^{-3}$ and $J_P = J_A = 1,000$.

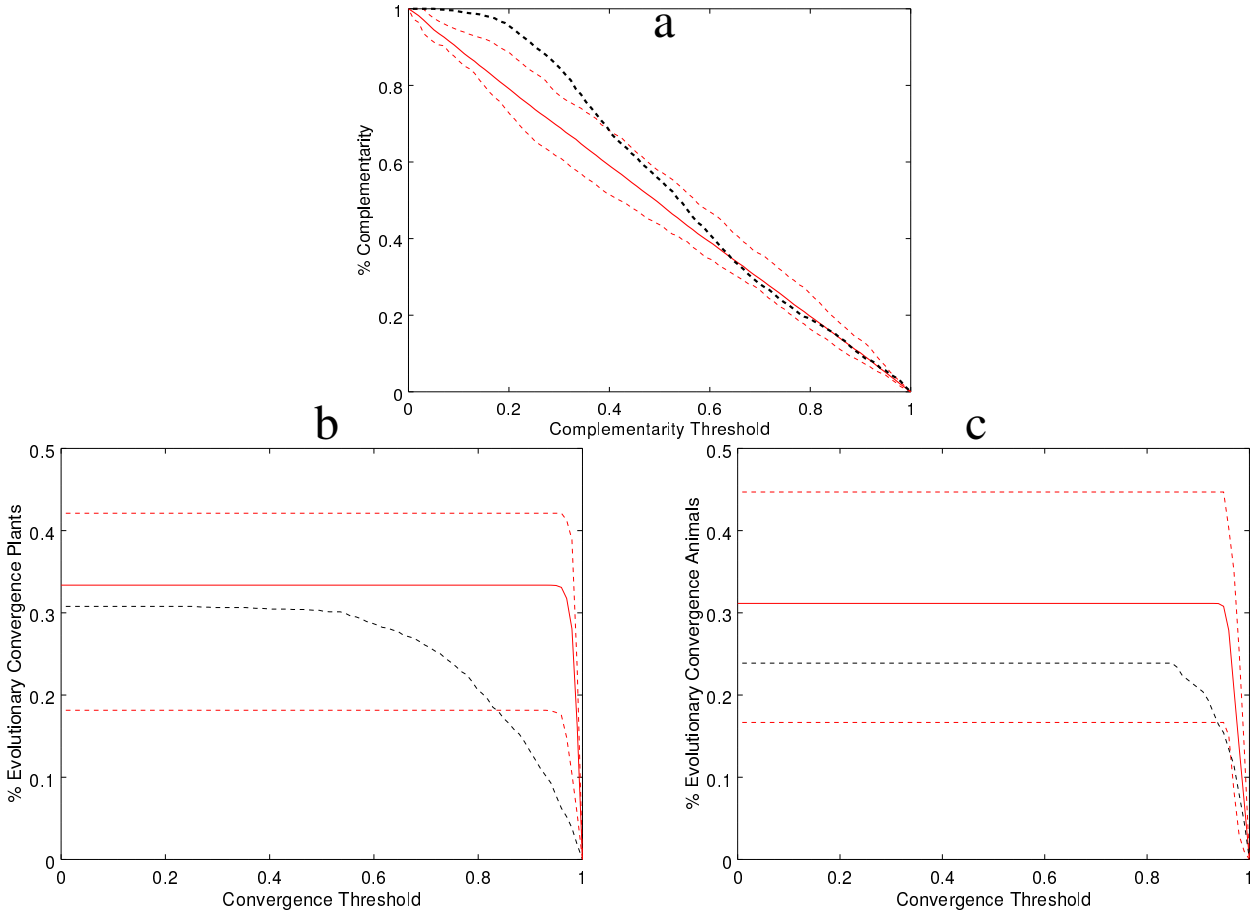

Figure 7: Comparison of model's predictions with estimations of convergence and complementarity from an empirical data of a plant-pollinator community. a) Shows the proportion of complementarity events (y-axis) as a function of the complementarity threshold (x-axis) for the empirical data (dotted black line) and for the model (continuous and dotted lines represent mean, 0.05 and 0.95 CI values, respectively). Predictions are within the CI for most complementarity threshold values. Empirical data deviates from model predictions for complementarity values around 0.4 and lower. b) Shows the proportion of convergence events in the plant community (y-axis, 69 species) as a function of the convergence threshold (x-axis) for the empirical data (dotted black line) and for the model (continuous and dotted lines represent mean, 0.05 and 0.95 CI values, respectively). Convergence events in the empirical data strongly deviates from model predictions for convergence threshold values ranging between 1 and 0.82. In that range, model predicts much higher proportion of convergence events than the empirical observations. c) Shows the proportion of convergence events in the animal community (y-axis, 24 species) as a function of the convergence threshold (x-axis) for the empirical data (dotted black line) and for the model (continuous and dotted lines represent mean, 0.05 and 0.95 CI values, respectively). Convergence events in the empirical data are within the CI of model predictions for most convergence threshold values.